

1 Adhesion of thiolated silica nanoparticles to urinary bladder mucosa: 2 Effects of PEGylation, thiol content and particle size

3
4 *Ellina A. Mun, Adrian C. Williams, Vitaliy V. Khutoryanskiy**

5 Reading School of Pharmacy, University of Reading, Whiteknights, Reading, RG6 6AD,
6 United Kingdom, email: v.khutoryanskiy@reading.ac.uk, Tel: +44(0)1183786119; fax:
7 +44 (0) 118 378 4703

8 9 10 ABSTRACT

11 Intravesical drug administration is used to deliver cytotoxic agents through a catheter to
12 treat bladder cancer. One major limitation of this approach is poor retention of the drug
13 in the bladder due to periodic urine voiding. Mucoadhesive dosage forms thus offer
14 significant potential to improve drug retention in the bladder. Here, we investigate
15 thiolated silica nanoparticles retention on porcine bladder mucosa *in vitro*, quantified
16 through Wash Out₅₀ (WO₅₀) values, defined as the volume of liquid necessary to
17 remove 50% of the adhered particles from a mucosal tissue. Following irrigation with
18 artificial urine solution, the thiolated nanoparticles demonstrate significantly greater
19 retention (WO₅₀ up to 36 mL) compared to non-mucoadhesive dextran (WO₅₀ 7 mL), but
20 have weaker mucoadhesive properties than chitosan (WO₅₀ 89 mL). PEGylation of
21 thiolated silica reduces their mucoadhesion with WO₅₀ values of 29 and 8 mL for
22 particles decorated with 750 and 5000 Da PEG, respectively. The retention of thiolated
23 silica nanoparticles is dependent on their thiol group contents and physical dimensions.

24

25 KEYWORDS: mucoadhesion, silica nanoparticles, PEGylation, intravesical drug
26 delivery, urinary bladder, thiomers, Wash Out₅₀ (WO₅₀)

27

28

29

30 1 INTRODUCTION

31 Urinary bladder cancer and interstitial cystitis are widespread and serious urological
32 conditions; bladder cancer is the ninth most common cancer in the world, with
33 approximately 430,000 new patients diagnosed with this condition in 2012 (WCRF,
34 2015). Intravesical drug delivery administers therapeutic agents directly into the urinary
35 bladder via a catheter (Malmstrom, 2003, Gasion and Cruz, 2006, Nirmal et al., 2012,
36 Haupt et al., 2013). This provides localized treatment, minimizes systemic side effects
37 and allows direct exposure of the affected tissue to therapeutic agents. However,
38 intravesical drug delivery also has some limitations. The normal capacity of the bladder
39 is 400–600 mL, but filling to 150–300 mL causes the urge to urinate. Due to periodical
40 voiding of urine from the bladder, instilled drug formulations can be rapidly washed out,
41 requiring frequent repeated administration (Guhasarkar and Banerjee, 2010).
42 Additionally, frequent use of catheters is inconvenient for the patients and may cause
43 inflammatory reactions and infections.

44 The residence time of a dosage form in the bladder can potentially be improved by
45 using mucoadhesive materials, which could adhere to the epithelial mucosa and resist
46 drug washout. Mucoadhesive formulations for intravesical drug delivery must satisfy
47 three main criteria: they should adhere rapidly to the bladder mucosa, should not

48 interfere with the normal functions of the bladder and should be retained *in situ* even
49 after urination (Tyagi et al., 2006).

50 Hydrophilic polymers are traditionally used as mucoadhesive materials in many
51 formulations for transmucosal drug delivery (Peppas, 1996; Andrews, 2009;
52 Khutoryanskiy, 2011) and commonly used are chitosan and carbomers (weakly cross-
53 linked poly(acrylic acid). The adhesion of these polymers to mucosal surfaces is through
54 non-covalent interactions such as hydrogen bonding, electrostatic attraction,
55 hydrophobic effects and diffusion and interpenetration (Khutoryanskiy, 2011). Recently,
56 a number of chemical approaches have been reported to enhance mucoadhesive
57 properties of polymers including the introduction of thiol groups (Bernkop-Schnürch,
58 2004), acrylate groups (Davidovich-Pinhas, 2011), catechols (Kim, 2015) and boronates
59 (Liu, 2015).

60 The literature contains few reports on chemically modified and enhanced mucoadhesive
61 materials for intravesical drug delivery. Barthelmes et al (2011, 2013) used thiolated
62 particles based on chitosan and demonstrated that retention in rat bladder *in vivo* was
63 approximately 170-fold greater than for a small-molecular weight fluorescent marker.
64 Storha et al (2013) developed thiolated nanoparticles using thiol-ene click chemistry and
65 studied their retention on porcine urinary bladder mucosa *in vitro*. Zhang et al (2014)
66 reported the synthesis of a series of β -cyclodextrin modified mesoporous silica
67 nanoparticles with hydroxyl, amino, and thiol groups. They demonstrated that retention
68 of thiol-functionalized nanoparticles on the urothelium was significantly higher than the
69 hydroxyl- and amino-functionalized materials.

70 Previously we have reported the synthesis of thiolated silica nanoparticles using self-
71 condensation of (3-mercaptopropyl)trimethoxysilane in dimethylsulfoxide
72 (Irmukhametova, 2011; Irmukhametova 2012; Mun, 2014a). These nanoparticles

73 exhibited strong adhesion to ocular tissues and withstood repetitive washes with
74 artificial tear fluid (Irmukhametova, 2011; Mun, 2014b). Here, we evaluate the retention
75 of thiolated and PEGylated silica nanoparticles on porcine urinary bladder *in vitro* and
76 show the effects of nanoparticle size on their mucoadhesive properties. Retention of the
77 nanoparticles depends on both their thiol content and dimensions. Further, we introduce
78 a novel quantitative method to compare the retention efficiency of liquid formulations on
79 mucosal tissues through the use of Wash Out₅₀ (WO₅₀) values, defined as the volume of
80 a biological fluid required to wash out 50% of a mucoadhesive formulation from a
81 substrate.

82

83 2 MATERIALS AND METHODS

84 2.1 GENERAL MATERIALS

85 (3-Mercaptopropyl)-trimethoxysilane (MPTS), dimethyl sulfoxide, dimethyl
86 formamide, acetonitrile, L-cysteine hydrochloride, 5,5'-dithiobis(2-nitrobenzoic acid), 5-
87 (iodoacetamido)-fluorescein, methoxypolyethylene glycol 750 Da maleimide,
88 methoxypolyethylene glycol 5000 Da maleimide, urea, chitosan (103 kDa), fluorescein
89 isothiocyanate (FITC) and fluorescein isothiocyanate dextran (FITC-dextran) were
90 purchased from Sigma-Aldrich (Gillingham, U.K.). Methanol was purchased from Fisher
91 Scientific Ltd (UK) and used as received.

92

93 2.2 SYNTHESIS OF THIOLATED SILICA NANOPARTICLES

94 Thiolated nanoparticles were synthesized according to our previously published
95 protocol (Mun, 2014b). Briefly, 0.75 mL (0.2 mol/L) or 0.38 mL (0.1 mol/L) of MPTS was
96 mixed with 20 mL of DMSO and 0.5 mL of 0.5 mol/L NaOH aqueous solution.

97 Additionally, the same procedure was repeated with 0.38 mL of MPTS in 20 mL of
98 dimethylformamide (DMF) and acetonitrile. The reaction was conducted with air
99 bubbling and allowed to proceed for 24 hours under constant stirring at room
100 temperature. Nanoparticles were purified by dialysis against deionized water (5L, 8
101 changes of water) using 12–14 kDa molecular weight cut off dialysis tubing (Medicell
102 International Ltd, UK).

103

104 2.3 ELLMAN'S ASSAY

105 Thiol-group content of the nanoparticles was determined by Ellman's assay. 0.2-0.3
106 mg of freeze-dried nanoparticles were hydrated in 500 μ L of phosphate buffer solution
107 (0.5mol/L, pH 8) and allowed to react with 500 μ L of 5,5'-dithio-bis-(2-nitrobenzoic acid)
108 (DTNB) for 2 hours. Absorbance was then measured at 420 nm (Epoch Microplate
109 Spectrophotometer, BioTek Instruments, USA). The calibration curve was constructed
110 with cysteine hydrochloride solutions over the concentration range of 25–175 μ mol/L (R^2
111 = 0.9998).

112

113 2.4 SYNTHESIS OF FLUORESCENTLY-LABELLED THIOLATED SILICA 114 NANOPARTICLES

115 Thiolated silica nanoparticles were labelled with 5-(iodoacetamido)-fluorescein (5-
116 IAF) by adding 3, 0.3, 0.4 and 0.05 mg of 5-IAF to 18, 20, 10 and 10 mL aqueous
117 dispersions of thiolated nanoparticles, respectively. The amount of 5-IAF added was
118 calculated with regard to molar ratios such that 5 μ mol of fluorophore was added to 50
119 μ mol of SH-groups of thiolated nanoparticles. The reaction mixture was stirred for 16
120 hours at room temperature protected from light. Fluorescently-labelled nanoparticles

121 were then purified by dialysis against deionized water in the dark, according to the
122 above protocol.

123 2.5 PEGYLATION OF FLUORESCENTLY-LABELLED SILICA NANOPARTICLES

124 5 mL aqueous dispersions of fluorescently-labelled nanoparticles were mixed with
125 100 mg of methoxypolyethylene glycol maleimide of two molecular weights (750 or 5000
126 Da). The reaction mixture was stirred during 16 hours at room temperature protected
127 from light, resulting in the formation of PEGylated silica nanoparticles. PEGylated
128 nanoparticles were purified by dialysis in the dark as above.

129

130 2.6 SYNTHESIS OF FLUORESCENTLY-LABELLED CHITOSAN

131 FITC-chitosan, used as a positive control for mucoadhesion tests, was
132 synthesized according to our previously published protocol (Cook, 2011). 1% w/v
133 chitosan solution was prepared in 100 mL of 0.1 mol/L acetic acid, followed by the
134 addition of 100 mL of dehydrated methanol and 50 mL of 2 mg/mL FITC solution in
135 methanol. The reaction was allowed to proceed for 3 hours in the dark at room
136 temperature and then precipitated in 1 L of 0.1 M NaOH. The precipitate was filtered
137 and dialyzed against 4 L of deionized water in the dark. The resulting product was
138 freeze-dried (Heto Power Dry LL 3000 freeze-drier, Thermo Electron Corporation) and
139 kept wrapped in aluminum foil to avoid exposure to light. For experiments, 0.05%
140 solutions of FITC-chitosan in 0.1 M acetic acid were used.

141 2.7 PREPARATION OF FLUORESCEIN ISOTHIOCYANATE DEXTRAN (4000 Da) 142 (FITC-DEXTRAN) SOLUTION

143 FITC-dextran solution, used as a negative control in mucoadhesion studies, was
144 prepared by dissolving 2 mg of FITC-dextran (4000 Da) in 10 mL of deionized water and
145 was left for 5 hours under permanent stirring at room temperature.

146 2.8 DYNAMIC LIGHT SCATTERING (DLS)

147 The size of fluorescently-labelled silica nanoparticles and their polydispersity (PDI)
148 values were determined by dynamic light scattering using a Nano-ZS series (Malvern
149 Instruments, UK) at 25°C. Each sample was analyzed three times from which the mean
150 \pm standard deviation hydrodynamic diameter values were calculated.

151

152

153 2.9 FLUORESCENCE SPECTROSCOPY

154 Fluorescence spectra were recorded for fluorescently-labelled thiolated and
155 PEGylated nanoparticles using a FP-6200 Spectrofluorometer (Jasco, UK) over the
156 wavelength range 505–700 nm ($\lambda_{\text{ex}}= 492$ nm).

157

158 2.10 PREPARATION OF ARTIFICIAL URINE SOLUTION

159 Artificial urine was prepared according to previously published protocol with slight
160 modifications (Chutipongtanate and Thongboonkerd, 2010). The following compounds
161 were dissolved in deionized water by stirring for 3 hours at room temperature, before
162 making the total volume to 2 L: urea (24.27 g), NaCl (6.34 g), KCl (4.50 g), NH₄Cl (1.61
163 g), CaCl₂ (0.67 g), MgSO₄•7H₂O (1.00 g), NaHCO₃ (0.34 g), Na₂SO₄ (0.26 g),
164 NaH₂PO₄•H₂O (1.00 g), and Na₂HPO₄ (0.11 g). The pH of the resulting solution was 6.2,

165 which is in agreement with Chutipongtanate and Thongboonkerd (2010). The artificial
166 urine solution was kept at 37° C throughout the experiments.

167 2.11 MUCOADHESION STUDIES USING PORCINE URINARY BLADDER

168 Mucoadhesive studies used a fluorescence microscope (Zeiss Imager A1) with an
169 AxioCam MRm Zeiss camera at 5 × magnification with 11.4 ms exposure time and 1388
170 × 1040 pixels. The porcine urinary bladders used in these experiments were obtained
171 from P.C. Turner Abattoir (Hampshire, UK). Freshly-extracted urinary bladders were
172 transported to the laboratory in a cold box and stored in the fridge at 4°C overnight prior
173 to retention studies. A sample of the bladder tissue (approximately 2 × 3 cm) was
174 carefully excised, avoiding contact with the mucosal side of the tissue, and was briefly
175 rinsed with ~3 mL of artificial urine solution. Experiments were performed with the
176 bladder tissue maintained at 37°C in a water bath. Background microscopy images
177 were recorded for each tissue sample prior to dosing with 200 µL of either fluorescently-
178 labelled nanoparticle dispersion or polymers (controls). Once the test material was
179 placed onto the mucosal surface, fluorescence microscopy images were again taken,
180 followed by 7 washing cycles, for each of which the bladder tissue was irrigated with 10
181 mL of artificial urine solution at 5 mL/min using a syringe pump. Fluorescence
182 microscopy images (3 for each sample) were recorded initially after treatment and after
183 each wash with the bladder tissue being placed onto a 75 mm x 25 mm glass slide.
184 Each experiment was conducted in triplicate. Microscopy images were analysed with
185 Image J software, the mean fluorescence values (fluorescence, a.u.) after each wash
186 were calculated and a histogram of fluorescence intensity distribution was presented as
187 a function of the volume of artificial urine solution used. The mean fluorescence values
188 were normalized by subtracting the background fluorescence provided by the bladder

189 tissue prior to exposing it to the test material and the initial (pre-wash) fluorescence was
190 taken as an intensity of 1.

191 Since the wash off experiments were not carried out in total darkness, to exclude the
192 possibility of the fluorophore bleaching with time, a portion of thiolated nanoparticles
193 dispersion was placed on the urinary bladder surface and fluorescence measured over
194 5 hours. Figure S1 shows that no significant decrease (Anova, Tukey's multiple
195 comparison's test, $p=0.2247$) in the fluorescence intensity of nanoparticle dispersion on
196 the bladder surface was observed over 5 hours, indicating their suitability for this type of
197 analysis.

198 WO_{50} values, representing the volume of artificial urine required to wash out 50% of the
199 particles, were calculated from the wash-off profiles. For example, WO_{50} values for
200 chitosan and dextran were calculated via extrapolation of the wash-off results to 50 %
201 using linear and exponential fits, respectively.

202

203

204 3 RESULTS AND DISCUSSION

205 3.1 SYNTHESIS AND CHARACTERIZATION OF FLUORESCENTLY-LABELLED 206 THIOLATED AND PEGYLATED SILICA NANOPARTICLES

207 Thiolated silica nanoparticles were synthesized using self-condensation of (3-
208 mercaptopropyl)trimethoxysilane (MPTS) in aprotic solvents in an oxidative environment
209 (bubbling with air) and with small portions of aqueous NaOH as a catalyst. Previously
210 (Mun, 2014b) we showed that the self-condensation of MPTS in dimethylsulfoxide forms
211 nanoparticles of 21 ± 1 nm and 45 ± 1 nm, when the concentration of MPTS in the feed

212 mixture was 0.1mol/L and 0.2 mol/L, respectively. These two types of nanoparticles
213 were also synthesized in the present study. Additionally, in this study we conducted the
214 reaction in other aprotic solvents, namely dimethylformamide (DMF) and acetonitrile
215 (AcN) for nanoparticle synthesis. Maintaining the MPTS at 0.1 mol/L, nanoparticles of
216 95 ± 14 and 217 ± 7 nm were produced in DMF and AcN, respectively. The effect of
217 aprotic solvent nature on the dimensions and properties of thiolated silica nanoparticles
218 has not been reported previously. By changing the concentration of MPTS in the feed
219 mixture and by changing the nature of aprotic solvent it is possible to make the thiolated
220 silica nanoparticles with a range of different sizes. It is widely recognized (Plumere et al,
221 2012) that formation of silica particles from alkoxysilanes (e.g. tetraalkoxysilane)
222 proceeds via several stages such as hydrolysis, condensation, nucleation, aggregation
223 and particle growth. The growth of primary particles as well as their further aggregation
224 are dependent on thermodynamic parameters of the system controlling their colloidal
225 stability. Polarity of the solvent is one of the factors affecting the particles at the
226 nucleation stage. Smaller particles are expected to form in solvents of greater polarity
227 (Wang et al, 2006), which was observed in this work.

228 All nanoparticles were fluorescently labelled by reacting with 5-(iodoacetamido)-
229 fluorescein (5-IAF). The fluorophore was added into the reaction mixture in a 5:50 μmol
230 ratio with regards to the number of SH-groups of silica nanoparticles; thus there were
231 still numerous thiol-groups available for mucoadhesion and for further functionalization.
232 The fluorescently labelled nanoparticles were characterized using dynamic light
233 scattering, fluorescent spectroscopy and Ellman's assay. Figure 1 shows size
234 distributions of the nanoparticles formed in DMSO, DMF and AcN, determined using
235 dynamic light scattering, illustrating the influence of changing solvent polarity on particle
236 size, but with similar dispersities.

237 Previously (Irmukhametova et al, 2011) it was demonstrated that PEGylation prevents
238 the adhesion of thiolated silica to intact bovine cornea, but could facilitate their
239 penetration into more porous stroma in de-epithelialized cornea (Mun et al, 2014).
240 Clearly, deeper penetration of particles into a biological tissue could also improve their
241 retention, which means that PEGylation may have various effects on particle behavior
242 on different mucosal surfaces. In this work the effect of thiolated silica PEGylation was
243 studied in relation of urinary bladder mucosa.

244 A portion of fluorescently-labelled thiolated nanoparticles synthesized in DMSO (45 ± 1
245 nm) was additionally reacted with PEG maleimide of two different molecular weights
246 (750 Da and 5000 Da) to generate two PEGylated silica nanoparticles. The general
247 characteristics of all silica nanoparticles synthesized in this work are summarized in
248 Table 1.

249

250 As expected, PEGylation generated larger nanoparticle size distributions, similar to our
251 previous findings (Mun, 2014b). The sizes of thiolated and PEGylated nanoparticles
252 were significantly different (ANOVA; Tukey's multiple comparisons test; $p<0.001$)
253 showing that the greater the molecular weight of PEG shell, the larger the nanoparticles.

254 PEGylation also reduced thiol groups content from 249 ± 30 $\mu\text{mol/g}$ to 95 ± 6 $\mu\text{mol/g}$ and
255 78 ± 5 $\mu\text{mol/g}$, when the nanoparticles were decorated with 750 Da and 5000 Da PEG,
256 respectively. Additionally, due to the screening effect of the PEG shells, reduced
257 fluorescence intensity was observed for PEGylated nanoparticles. PEG of a larger
258 molecular weight provided the lowest fluorescence intensity, since screening with PEG
259 5000 Da is greater than with PEG 750 Da. For thiolated samples prepared in different
260 solvents, the lowest fluorescence intensity was observed for those synthesized in

261 acetonitrile, which contained the lowest amount of SH-groups on their surface and
262 hence a lower quantity of the fluorophore conjugated.

263

264

265 3.2 COMPARATIVE MUCOADHESION STUDIES OF THIOLATED AND PEGYLATED 266 NANOPARTICLES

267 Bernkop-Schnurch introduced thiolated polymers (thiomers) as a new generation of
268 mucoadhesive materials (Bernkop-Schnurch, 2005). Thiomers exhibit enhanced
269 mucoadhesion compared to their unmodified parent polymers due to the formation of
270 disulfide bridges (covalent bonds) between thiol-groups of the polymer and cysteine-rich
271 domains of mucus glycoproteins. Barthelmes et al. (2011) reported the synthesis of
272 chitosan-thioglycolic acid nanoparticles, loaded with trimethoprim, for targeted drug
273 release in the urinary bladder. These nanoparticles enabled controlled and sustainable
274 drug release, showed greater stability and superior mucoadhesion compared to
275 unmodified chitosan particles. The presence of thiol groups on the surface of silica
276 nanoparticles also makes them promising as mucoadhesive materials for application in
277 drug delivery.

278 The retention of fluorescently-labelled thiolated and PEGylated silica nanoparticles on
279 porcine urinary bladder mucosa was studied using a flow-through method with
280 fluorescent detection (Irmukhametova, 2011; Storha, 2013; Withers, 2013). Figure 2
281 shows representative fluorescent images of the retention of thiolated and PEGylated
282 silica as well as two controls (chitosan and dextran) on urinary bladder mucosa, washed
283 with artificial urine. Fluorescently-labelled chitosan was selected as a positive control
284 because it is a cationic polymer with well-documented ability to adhere to mucosal

285 surfaces (Sogias et al., 2008, Khutoryanskiy, 2011). Fluorescently-labelled dextran, on
286 the contrary, had very poor adhesion to mucosal surfaces (Storha, 2013; Withers,
287 2013), and so was used as a negative control in our experiments.

288 Analysis of the fluorescent images using ImageJ software allows the retention of
289 fluorescent species on mucosal surfaces to be quantified (Figure 3). FITC-chitosan is
290 retained on the bladder surface even after 7 washes (total volume 70 mL) with artificial
291 urine solution and illustrates its strong interaction with the mucosal surface. However,
292 for FITC-dextran, a significant decrease in fluorescence was observed after the first
293 wash (10 mL) with urine solution, confirming its poor mucoadhesive properties.

294

295

296 Retention of thiolated silica nanoparticles on the bladder mucosa was significantly
297 higher than for FITC-dextran ($p < 0.05$): approximately 15% of the fluorescence, hence
298 particles, remains on the mucosal surface even after 7 washing cycles with 10 mL of
299 artificial urine solution. However, their retention was significantly lower than FITC-
300 chitosan ($p < 0.05$). This may be due to the polymeric nature of chitosan, whose
301 positively-charged macromolecules are able to penetrate into the mucosal layer of the
302 bladder epithelium, form non-covalent interactions (e.g. electrostatic attraction and
303 hydrogen bonding) with mucins and generate an interpenetration layer (Sogias, 2008).
304 This interpenetration could potentially facilitate better retention of chitosan on the
305 bladder mucosa compared to thiolated nanoparticles.

306 PEGylated silica nanoparticles were washed from the mucosal surface more rapidly
307 than the thiolated parent particles and hence are less mucoadhesive. The normalized
308 fluorescence intensity of PEGylated (750 Da) nanoparticles on the bladder surface was

309 similar (T-test, $p=0.8937$) to that of its thiolated counterpart after the first wash. Whilst
310 the thiolated nanoparticles stayed on the bladder surface after 7 washes, PEGylated
311 (750 Da) nanoparticles were completely removed after 6 washes. PEGylated (5000 Da)
312 nanoparticles revealed poorer retention than when modified with 750 Da PEG and were
313 removed after 5 washes, similar to the negative control, FITC-dextran. Weaker retention
314 for the PEGylated (5000 Da) silica relates to greater screening of the surface thiol
315 groups by the larger molecular weight polymer and to the thiol content on the
316 nanoparticle surface itself (Table 1).

317 The poorer mucoadhesive performance of PEGylated nanoparticles compared to the
318 thiolated silica is in good agreement with our previous study of retention of similar
319 nanoparticles on the ocular surfaces (Irmukhametova, 2011). However, both thiolated
320 and PEGylated (5000 Da) nanoparticles in our previous report demonstrated a very
321 sharp drop in fluorescence intensity (of 62% and 95%, respectively) after the first wash
322 and the PEGylated nanoparticles were removed from the ocular surface after three
323 washes. Here, PEGylated (PEG 5000 Da) nanoparticles were removed from the bladder
324 mucosa after 6 wash cycles. This discrepancy can be explained by the different nature
325 of two mucosal tissues (Irmukhametova et al., 2011); the rougher structure of the
326 bladder epithelium compared to the cornea provides better retention of silica
327 nanoparticles on its mucosal surface.

328 Retention studies were conducted with differing sizes of thiolated silica nanoparticles,
329 synthesized in different aprotic solvents (DMSO, DMF and AcN, Table 1). Figure 4
330 shows the retention profiles for these nanoparticles.

331

332 The greatest retention in this series is observed for 21 ± 1 nm thiolated nanoparticles,
333 synthesized in DMSO: they remain on the surface of the bladder mucosa for up to 6-7
334 washes with 10 mL of artificial urine. The nanoparticles synthesized in DMF are much
335 larger (95 ± 14 nm), but have similar thiol content as the thiolated silica prepared in
336 DMSO (119 ± 12 $\mu\text{mol/g}$ and 118 ± 14 $\mu\text{mol/g}$, respectively). Their retention on the bladder
337 mucosa is poorer and no traces of these nanoparticles are detectable after 7 wash
338 cycles. This clearly indicates that the nanoparticles of larger size have weaker retention
339 on the bladder mucosa, which is possibly related to their poorer ability to penetrate into
340 the mucosal layer. The weakest retention on the bladder mucosa was observed for the
341 thiolated silica, synthesized in AcN. Both their large size (217 ± 7 nm) and low SH-groups
342 content (40 ± 6 $\mu\text{mol/g}$) could contribute to this poor mucoadhesive performance.

343 A comparison between the nanoparticles synthesized in DMSO from the feed mixtures
344 containing different quantities of MPTS reveals that the thiolated silica of 45 ± 1 nm
345 (Figure 3) retains on the bladder mucosa better than 21 ± 1 nm nanoparticles (Figure 4).
346 This is explained by the greater thiol content (249 ± 30 $\mu\text{mol/g}$) of the 45 ± 1 nm particles
347 compared to 21 ± 1 nm material which had a lower concentration of SH-groups (118 ± 14
348 $\mu\text{mol/g}$).

349 Direct quantitative comparisons between different wash-off profiles is problematic
350 unless each set of data could be converted into a simple numerical value. To this end,
351 we propose WO_{50} values, which represent the volume of a biological fluid required to
352 wash out 50% of the mucoadhesive ingredient from a substrate surface. These values
353 were calculated by analyzing individual wash-off profiles and the results are
354 summarized in Table 1. By comparing these values for different particles used in this
355 study, it is clear that the greatest retention is observed for 45 ± 1 nm thiolated silica
356 particles with the highest SH-groups content (249 ± 30 $\mu\text{mol/g}$), whose WO_{50} is 36 mL.

357 PEGylation of these particles reduces their retention with WO_{50} values dropping to 29
358 and 8 mL for 750 Da and 5000 Da PEG, respectively. Thiolated nanoparticles have
359 greater retention on bladder mucosa compared to non-mucoadhesive dextran (WO_{50} 7
360 mL), but have weaker mucoadhesive properties than chitosan (WO_{50} 89 mL).

361 The smallest thiolated particles of 21 ± 1 nm diameter have a lower SH-groups content
362 (118 ± 14 $\mu\text{mol/g}$) than those of 45 ± 1 nm diameter and showed an expectedly lower
363 WO_{50} of 17 mL. However, the nanoparticles synthesized in DMF are larger (95 ± 14 nm),
364 have a similar SH-groups content (119 ± 12 $\mu\text{mol/g}$) but are more readily washed from
365 the tissue (WO_{50} 7mL). Hence the retention of particles on mucosal surfaces is not only
366 dependent on their surface thiol-groups but also on their size. Indeed, the largest
367 thiolated particles synthesized in acetonitrile (217 ± 7 nm) have the lowest SH-groups
368 content (40 ± 6 $\mu\text{mol/g}$) and exhibit weakest retention on mucosal surfaces ($WO_{50} = 6$
369 mL).

370

371 4.4 CONCLUSIONS

372 The retention of thiolated and PEGylated silica nanoparticles on porcine urinary
373 bladder mucosa has been studied *in vitro* using fluorescence microscopy. It was shown
374 that the thiolated nanoparticles adhere well to bladder mucosa and withstand wash out
375 effects caused by urine. Retention of these nanoparticles depends on their thiol-content
376 and dimensions. PEGylation of thiolated silica greatly reduces their mucoadhesive
377 properties. The use of WO_{50} values, introduced in this work, provides a convenient
378 method to quantitatively compare the retention of particulates and other materials on
379 differing mucosal surfaces and between differing research protocols.

380

381 ACKNOWLEDGEMENTS:

382 We thank the Leverhulme Trust for funding the *in vitro* retention experiments in this
383 study (RPG-2013-017). EAM is grateful to University of Reading for International
384 Postgraduate Research Studentship. The authors are grateful to P.C. Turner Abattoir
385 (Hampshire, UK) for providing pig bladders for experiments. Dr P. Morrison is
386 acknowledged for the prompt delivery of biological tissues.

387

388

389 REFERENCES:

390 Andrews G.P., Lavery T.P., Jones D.S. (2009) Mucoadhesive polymeric platforms for
391 controlled drug delivery. *European Journal of Pharmaceutics and Biopharmaceutics* 71,
392 505–518

393

394 Barthelmes J., Perera G., Hombach J., Dünnhaupt S., Bernkop-Schnurch A. (2011)
395 Development of a mucoadhesive nanoparticulate drug delivery system for a targeted
396 drug release in the bladder. *International Journal of Pharmaceutics* 416, 339–345

397

398 Barthelmes J., Dünnhaupt S., Unterhofer S., Perera G., Schlocker W., Bernkop-
399 Schnürch A. (2013) Thiolated particles as effective intravesical drug delivery systems
400 for treatment of bladder-related diseases. *Nanomedicine* 8, 65-75.

401

402 Bernkop-Schnurch A. (2005) Thiomers: A new generation of mucoadhesive polymers.
403 *Advanced Drug Delivery Reviews* 57, 1569–1582

404

405 Chutipongtanate S., Thongboonkerd V. (2010) Systematic comparisons of artificial urine
406 formulas for in vitro cellular study. *Analytical Biochemistry* 402, 110–112
407

408 Cook M.T., Tzortzis G., Charalampopoulos D. and Khutoryanskiy V.V. (2011)
409 Production and Evaluation of Dry Alginate-Chitosan Microcapsules as an Enteric
410 Delivery Vehicle for Probiotic Bacteria. *Biomacromolecules* 12, 2834–2840
411

412 Davidovich-Pinhas M. and Bianco-Peled H. (2011) Physical and structural
413 characteristics of acrylated poly(ethylene glycol)-alginate conjugates, *Acta Biomaterialia*
414 7, 2817-2825.
415

416 Gasion J.P.B., Cruz J.F.J. (2006) Improving efficacy of intravesical chemotherapy.
417 *European Urology* 50, 225–234
418

419 Guhasarkar S. and Banerjee R. (2010) Intravesical drug delivery: challenges, current
420 status, opportunities and novel strategies. *Journal of Controlled Release* 148, 147–159
421

422 Haupt M., Thommes M., Heidenreich A., Breitzkreutz J (2013) Lipid-based intravesical
423 drug delivery systems with controlled release of trospium chloride for the urinary
424 bladder. *Journal of Controlled Release* 170, 161–166
425

426 Irmukhametova G.S., Mun G.A., and Khutoryanskiy V.V. (2011) Thiolated
427 mucoadhesive and PEGylated non-mucoadhesive organosilica nanoparticles from 3-
428 mercaptopropyltrimethoxysilane. *Langmuir* 27, 9551–9556
429

430 Irmukhametova G.S., Fraser B., Keddie J.L., Mun G.A., Khutoryanskiy V.V. (2012)
431 Hydrogen-Bonding-Driven Self-Assembly of PEGylated Organosilica Nanoparticles with
432 Poly(acrylic acid) in Aqueous Solutions and in Layer-by-Layer Deposition at Solid
433 Surfaces, *Langmuir*, 28, 299-306
434
435 Khutoryanskiy V.V. (2011) Advances in mucoadhesion and mucoadhesive polymers.
436 *Macromolecular Bioscience* 11, 748–764
437
438 Kim K., Kim K., Ryu J.H., Lee H. (2015) Chitosan-catechol: A polymer with long-lasting
439 mucoadhesive properties, *Biomaterials* 52, 161–170
440
441 Liu S., Chang C.N., Verma M.S., Hileeto D., Muntz A., Stahl U., Woods J., Jones L.W.,
442 Gu F.X. (2015) Phenylboronic acid modified mucoadhesive nanoparticle drug carriers
443 facilitate weekly treatment of experimentally induced dry eye syndrome. *Nano Research*
444 8, 621-635
445
446 Malmstrom P-U. (2003) Intravesical therapy of superficial bladder cancer. *Critical*
447 *Reviews in Oncology/Hematology* 47, 109–126
448
449 Mun E.A., Hannell C., Rogers S.E., Hole P., Williams A.C., Khutoryanskiy V.V. (2014a)
450 On the role of specific interactions in the diffusion of nanoparticles in aqueous polymer
451 solutions, *Langmuir*, 30, 308-317
452
453 Mun E.A., Morrison P.W.J., Williams A.C., Khutoryanskiy V.V. (2014b) On the barrier
454 properties of the cornea: A microscopy study of the penetration of fluorescently labelled
455 nanoparticles, polymers, and sodium fluorescein. *Mol. Pharm.*, 11, 3556-3564

456 Nirmal J., Chuang Y-C., Tyagi P., Chancellor M.B. (2012) Intravesical therapy for lower
457 urinary tract symptoms. *Urological Science* 23, 70–77
458

459 Peppas N.A. and Sahlin J.J. (1996) Hydrogels as mucoadhesive and bioadhesive
460 materials: a review. *Biomaterials* 17, 1553–1561
461

462 Plumere N., Ruff A., Speiser B., Feldmann, Mayer H.A. (2012) Stober silica particles as
463 basis for redox modifications: Particle shape, size, polydispersity, and porosity. *Journal*
464 *of Colloid and Interface Science*, 368, 208-219.
465

466 Sogias I.A., Williams A.C., and Khutoryanskiy V.V. (2008) Why is chitosan
467 mucoadhesive? *Biomacromolecules* 9, 1837–1842
468

469 Storha A., Mun E.A. and Khutoryanskiy V.V. (2013) Synthesis of thiolated and acrylated
470 nanoparticles using thiol-ene click chemistry: towards novel mucoadhesive materials for
471 drug delivery. *RSC Advances* 3, 12275–12279
472

473 Tyagi P., Wu P-C., Chancellor M., Yoshimura N., and Huang L. (2006) Recent
474 advances in intravesical drug/gene delivery. *Molecular Pharmaceutics* 3, 369–379
475

476 Wang H.-C., Wu C.-Y., Chung C.-C., Lai M.-H., Chung T.-W. (2006) Analysis of
477 parameters and interaction between parameters in preparation of uniform silicon dioxide
478 nanoparticles using response surface methodology. *Industrial and Engineering*
479 *Chemistry Research* 45, 8043-8048
480

481 WCRF (2015) [http://www.wcrf.org/int/cancer-facts-figures/data-specific-](http://www.wcrf.org/int/cancer-facts-figures/data-specific-cancers/bladder-cancer-statistics)
482 [cancers/bladder-cancer-statistics](http://www.wcrf.org/int/cancer-facts-figures/data-specific-cancers/bladder-cancer-statistics), accessed 17 May 2015

483

484 Withers C.A., Cook M.T., Methven L., Gosney M.A., Khutoryanskiy V.V. (2013)
485 Investigation of milk proteins binding to the oral mucosa, Food & Function, 4, 1668–
486 1674

487

488 Zhang Q., Neoh K.G., Xu L., Lu S., Kang E.T, Mahendran R., Chiong E. (2014)
489 Functionalized Mesoporous Silica Nanoparticles With Mucoadhesive and Sustained
490 Drug Release Properties for Potential Bladder Cancer Therapy. Langmuir 30, 6151-
491 6161.

492

493

494

495

496

Captions to figures

497 Figure 1. Size distribution of thiolated silica nanoparticles, fluorescently-labelled with 5-
498 IAF

499 Figure 2. Exemplar fluorescence microphotographs showing retention of FITC-chitosan,
500 thiolated silica, PEGylated silica (750 Da), PEGylated silica (5000 Da) and FITC-dextran
501 on porcine urinary bladder mucosa as washed with different volumes of artificial urine
502 solution. Scale bar is 200 μm .

503 Figure 3. Fluorescence intensities showing retention of FITC-chitosan, thiolated silica,
504 PEGylated silica (750 Da), PEGylated silica (5000 Da) and FITC-dextran on porcine
505 urinary bladder mucosa after washing with different volumes of artificial urine solution.
506 Each experiment was performed in triplicate and results are presented as the mean
507 value \pm standard deviation. Initial intensity after dosing is taken as a value of 1.

508 Figure 4. Fluorescence levels showing retention of thiolated silica nanoparticles
509 synthesized in DMSO, DMF and AcN on the urinary bladder surface washed with
510 artificial urine. Each experiment was performed in triplicate and the results are
511 presented as the mean value \pm standard deviation.

512

513

514 Table 1. Characteristics of fluorescently-labelled thiolated and PEGylated silica
515 nanoparticles

Sample	Diameter, nm	PDI	Nanoparticle concentration, mg/mL	[SH], $\mu\text{mol/g}$	WO ₅₀ *, mL
Thiolated (DMSO + 0.2 mol/L MPTS)	45±1	0.332	5	249±30	36
PEGylated (750 Da)	54±1	0.194	5	95±6	29
PEGylated (5000 Da)	69±2	0.145	7	78±5	8
Thiolated (DMSO + 0.1 mol/L MPTS)	21±1	0.263	4	118±14	17
Thiolated (DMF + 0.1 mol/L MPTS)	95±14	0.310	4	119±12	7
Thiolated (AcN+ 0.1 mol/L MPTS)	217±7	0.056	3	40±6	6

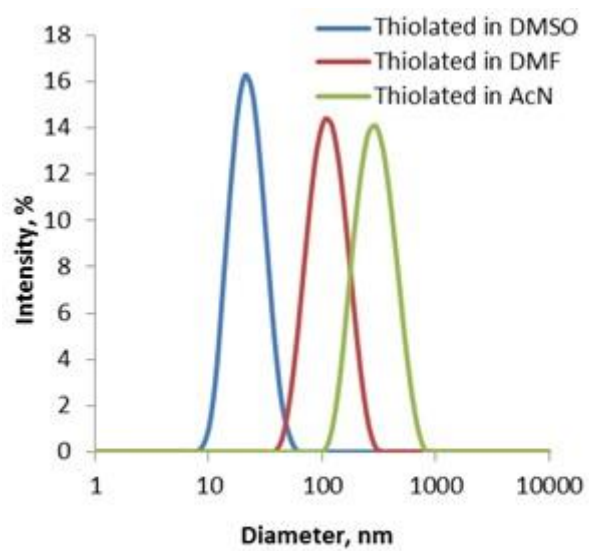
516 * WO₅₀ is the volume of artificial urine required to wash out 50% of the particles

517

518

519

520

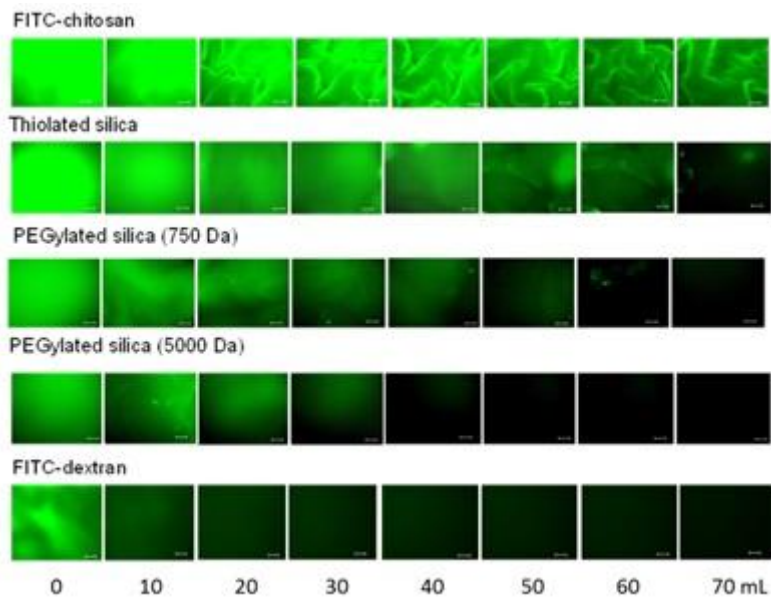


521

522 Figure 1

523

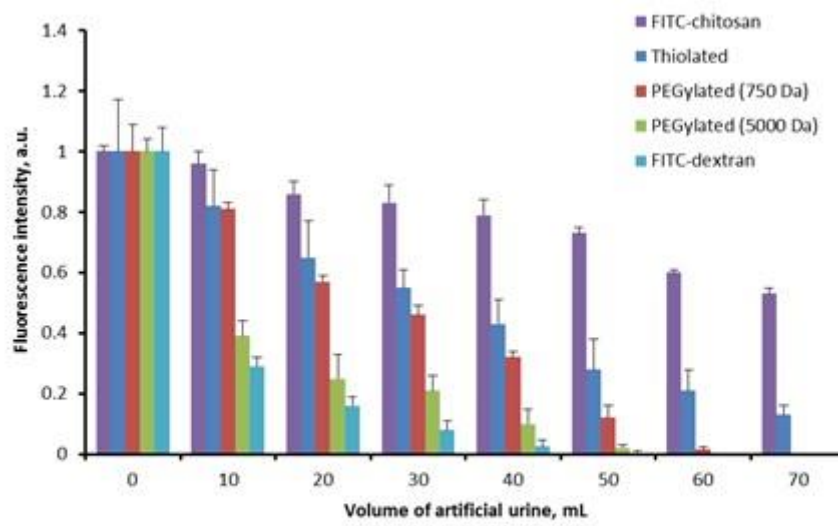
524



525

526 Figurte 2

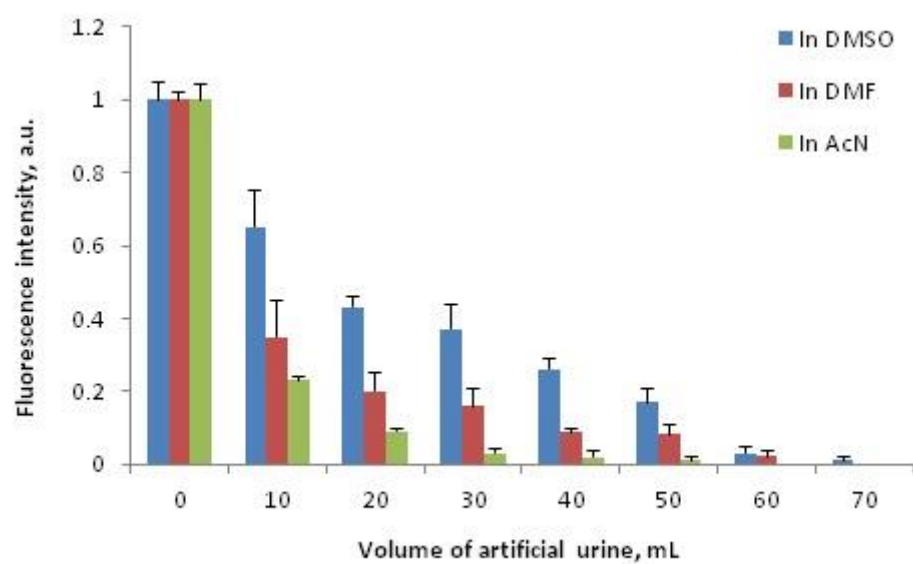
527



528

529 Figure 3

530



531

532 Figure 4

533

534